

## Supporting information

# Excited state interactions between the chiral Au<sub>38</sub>L<sub>24</sub> cluster and covalently attached porphyrin

Birte Varnholt,<sup>a</sup> Romain Letrun,<sup>a</sup> Jesse Bergkamp,<sup>b</sup> Yongchun Fu,<sup>b</sup> Oleksandr Yushchenko,<sup>a</sup> Silvio Decurtins,<sup>b</sup> Eric Vauthey,<sup>a</sup> Shi-Xia Liu,<sup>b</sup> Thomas Bürgi<sup>a\*</sup>

<sup>a</sup> Department of Physical Chemistry, University of Geneva, Quai Ernest Ansermet 30, 1211 Geneva, Switzerland. E-mail: Thomas.buergi@unige.ch

<sup>b</sup> Department of Chemistry and Biochemistry, University of Berne, Freiestrasse 3, 3012 Berne, Switzerland.

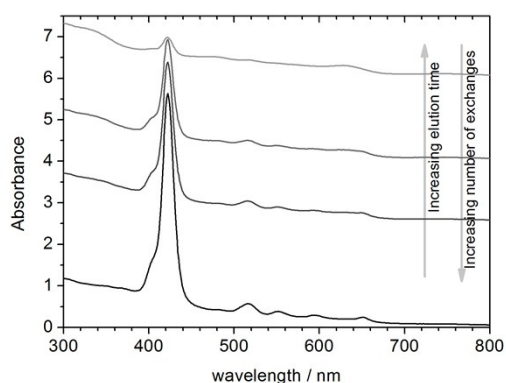


Fig. S 1: UV-vis spectra (normalized to 350 nm) of fractions separated by size exclusion chromatography. Ligand-exchanged clusters elute first, due to the significant increase in size when the large porphyrin (relative to the clusters size) is attached.

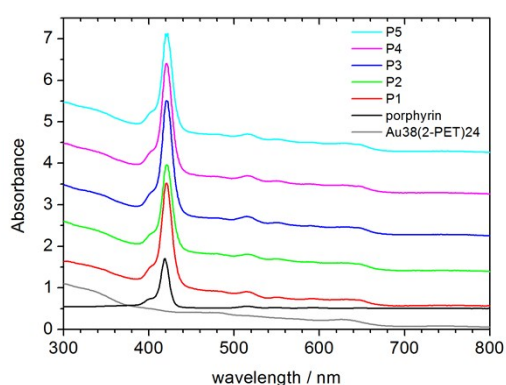


Fig. S 2: UV-vis spectra (normalized to 350 nm and shifted for clarity) of HPLC isolated fractions. All spectra show the same features of porphyrin and Au<sub>38</sub>L<sub>24</sub> absorption bands.

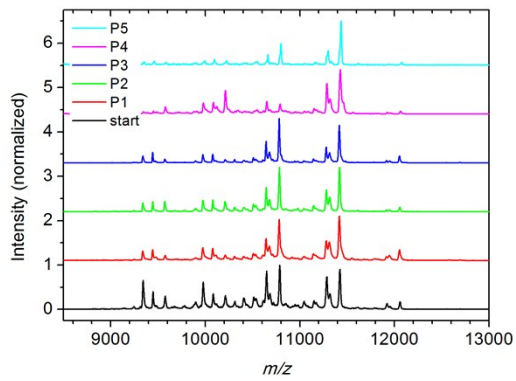


Fig. S 3: MALDI spectra from HPLC collected samples show non-exchanged ( $m/z = 10778$ ), mono- ( $m/z = 11413$ ) and small amounts of biexchanged ( $m/z = 12048$ ) clusters

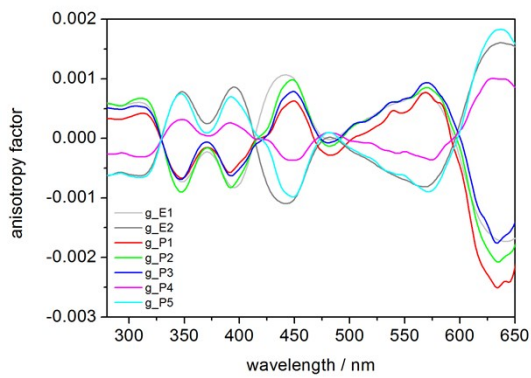


Fig. S 4: Calculated anisotropy factor ( $g = \Delta A / A$ ) for the fraction separated by HPLC. The value lies in the same order of magnitude as for pure enantioseparated  $\text{Au}_{38}(\text{2PET})_{24}$ .

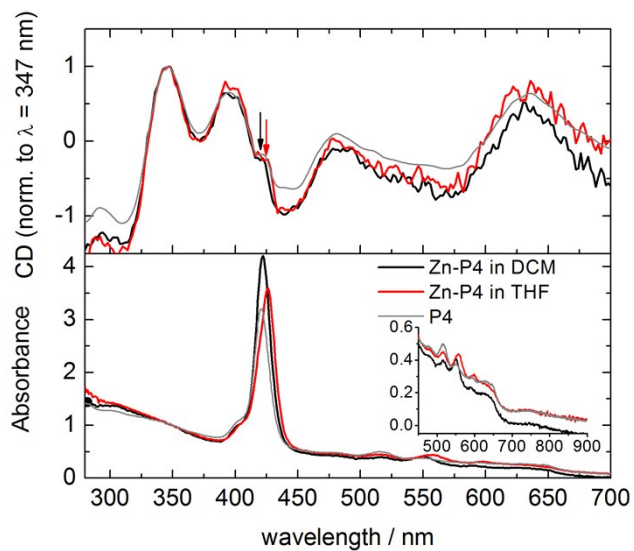


Fig. S 5: UV-vis and CD spectra of fraction P4 after  $\text{Zn}^{2+}$  incorporation measured in dichloromethane (DCM) and tetrahydrofuran (THF).

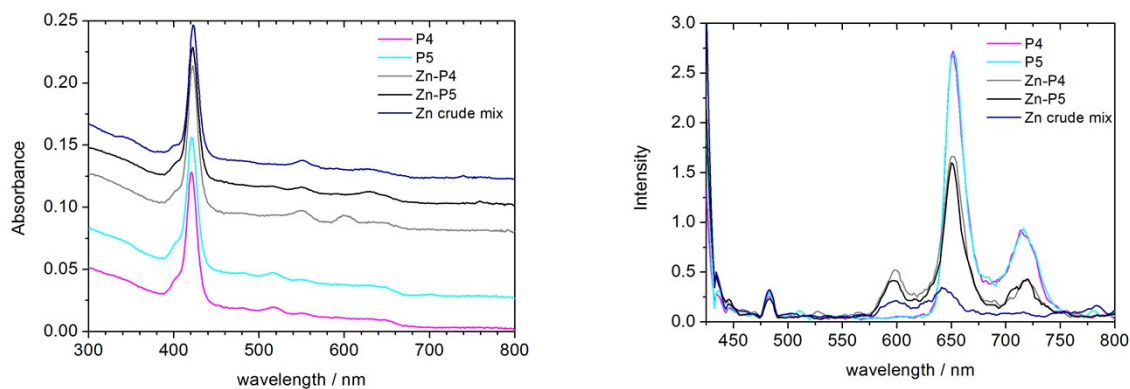


Fig. S 6: Fluorescence and absorption spectra of fractions P4 and P5 after incorporation of Zn. A typical blue shift of the emission bands is observed.

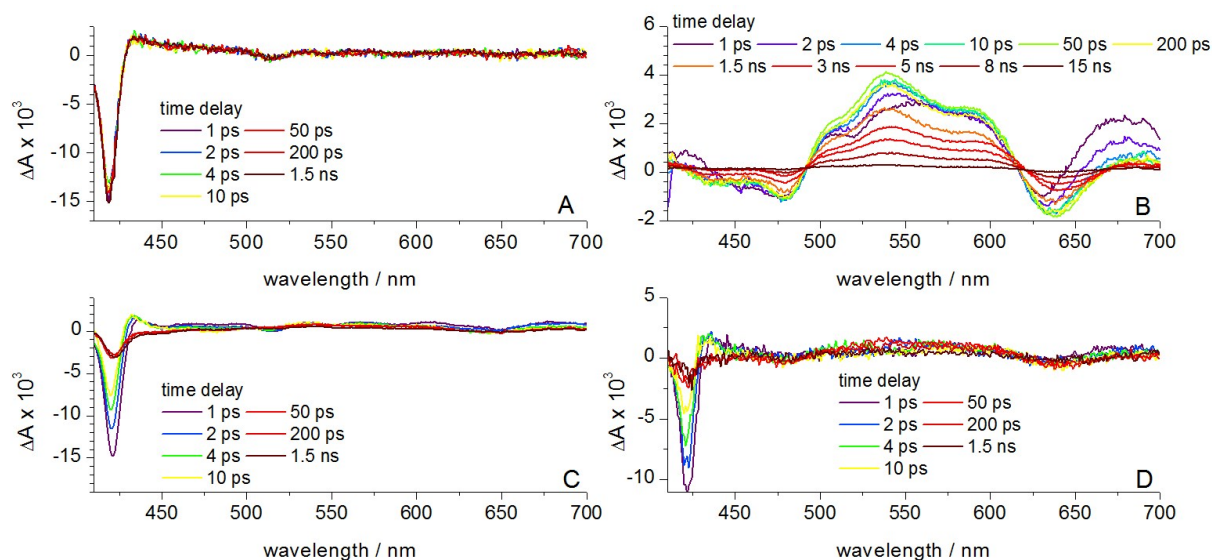


Fig. S 7: Transient absorption spectra of (A) free base porphyrin, (B)  $\text{Au}_{38}(\text{2PET})_{24}$ , (C)  $\text{Au}_{38}(\text{2PET})_{24-n}(\text{porphyrin})_n$  ( $n = 0-2$ ) and (D)  $\text{Au}_{38}(\text{2PET})_{24n}(\text{Zn-porphyrin})_n$  ( $n = 0-2$ ) in DCM. Spectra 1 ps to 1.5 ns were measured after excitation at 400 nm while for the spectra 3 ns to 15 ns an excitation wavelength 355 nm was used.

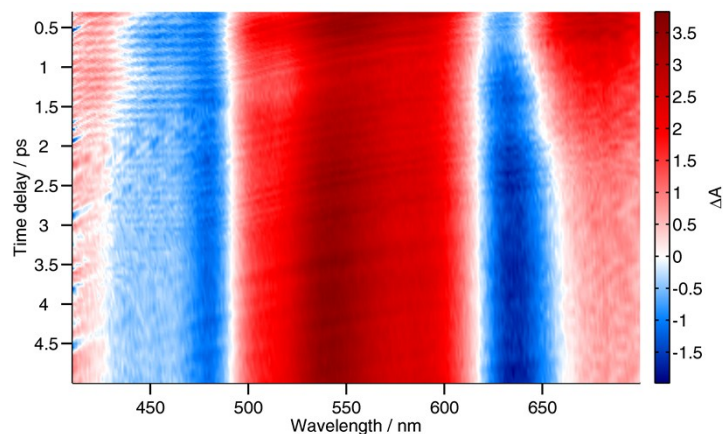


Fig. S 8: 2D map of the transient absorption data measured with  $\text{Au}_{38}(\text{2PET})_{24-n}(\text{porphyrin})_n$  ( $n = 0-2$ ) in DCM.

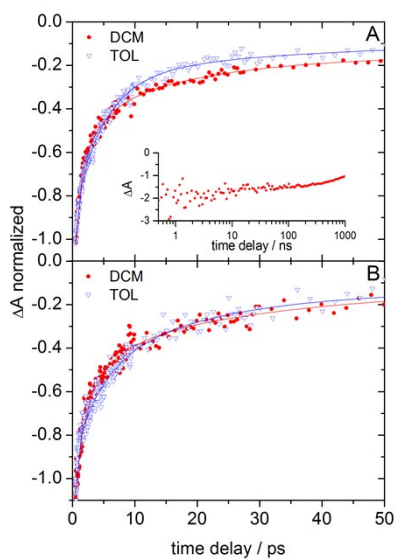


Fig. S 9: Temporal evolution of the Soret band ground-state bleach (averaged between 420 and 422 nm) for  $\text{Au}_{38}(\text{2PET})_{24-n}(\text{porphyrin})_n$  ( $n = 0-2$ ) (A) and  $\text{Au}_{38}(\text{2PET})_{24-n}(\text{Zn-porphyrin})_n$  ( $n = 0-2$ ) (B) measured upon 400 nm excitation. Solid lines are fit to the data. The inset in (A) shows the evolution on a longer time scale, in DCM, measured upon 532 nm excitation.

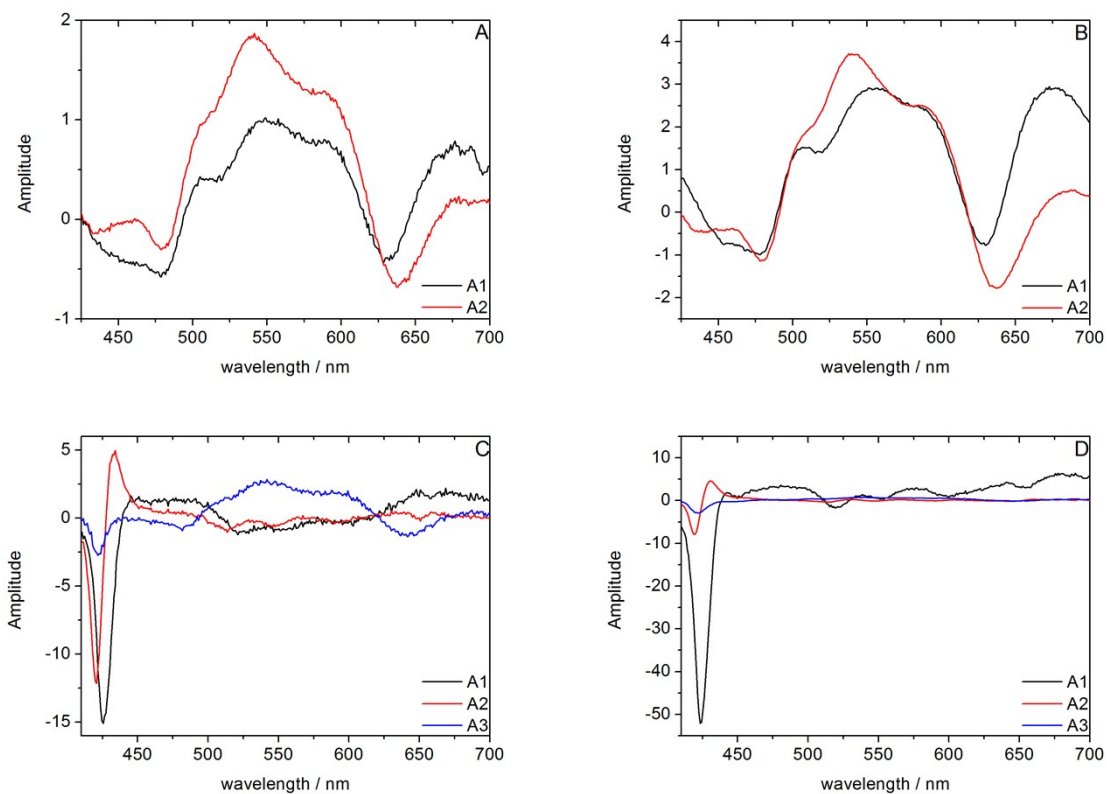


Fig. S 10: Decay-associated difference spectra obtained from the global analysis of the TA spectra A (B)  $\text{Au}_{38}(\text{2PET})_{24}$  in toluene ( dichloromethane) and C (D) porphyrin functionalized cluster in toluene (dichloromethane).